



This is a repository copy of *Very high gain and low noise GaAsSb/AlGaAsSb avalanche photodiodes for 1550nm detection at room temperature.*

White Rose Research Online URL for this paper:

<https://eprints.whiterose.ac.uk/220633/>

Version: Published Version

Proceedings Paper:

Liu, Y. orcid.org/0000-0003-3034-9628, Jin, X. orcid.org/0000-0002-7205-3318, Lee, S. et al. (10 more authors) (2024) Very high gain and low noise GaAsSb/AlGaAsSb avalanche photodiodes for 1550nm detection at room temperature. In: Jiang, S. and Digonnet, M.J., (eds.) Optical Components and Materials XXI. Optical Components and Materials XXI, 27 Jan - 01 Feb 2024, San Francisco, California, United States. Society of Photo Optical Instrumentation Engineers (SPIE) ISBN 9781510670242

<https://doi.org/10.1117/12.3011687>

© 2024 Society of Photo Optical Instrumentation Engineers (SPIE). One print or electronic copy may be made for personal use only. Systematic reproduction and distribution, duplication of any material in this publication for a fee or for commercial purposes, or modification of the contents of the publication are prohibited.

Reuse

Items deposited in White Rose Research Online are protected by copyright, with all rights reserved unless indicated otherwise. They may be downloaded and/or printed for private study, or other acts as permitted by national copyright laws. The publisher or other rights holders may allow further reproduction and re-use of the full text version. This is indicated by the licence information on the White Rose Research Online record for the item.

Takedown

If you consider content in White Rose Research Online to be in breach of UK law, please notify us by emailing eprints@whiterose.ac.uk including the URL of the record and the reason for the withdrawal request.



eprints@whiterose.ac.uk
<https://eprints.whiterose.ac.uk/>

VERY HIGH GAIN AND LOW NOISE GaAsSb/AlGaAsSb AVALANCHE PHOTODIODES FOR 1550NM DETECTION AT ROOM TEMPERATURE

Yifan Liu^{a*}, Xiao Jin^{a*}, Seunghyun Lee^b, Hyemin Jung^b, Harry I. J. Lewis^a, Bingtian Guo^c, Sri H. Kodati^b, Mariah Schawrtz^b, Christopher Grein, T.J. Ronningen^b, Joe C. Campbell^c, Sanjay Krishna^b and John P. R. David^a

^a Department of Electronic and Electrical Engineering, The University of Sheffield, Sheffield, S1 3JD, UK

^b Department of Electrical and Computer Engineering, The Ohio State University, Columbus, Ohio 43210, USA

^c Department of Electrical and Computer Engineering, University of Virginia, Charlottesville, Virginia 22904, USA

^d Department of Physics, University of Illinois, Chicago, Illinois 60607, USA

*These authors contributed equally to this work

Corresponding author: Xiao Jin (xjin4@outlook.com) and John David (j.p.david@sheffield.ac.uk)

1. ABSTRACT

The performance of the photodetector is often the primary limiting factor affecting a free space communication or LiDAR system's sensitivity. Avalanche photodiodes (APDs) can be used to improve the signal to noise ratio (SNR) compared to conventional *p-i-n* photodiodes. Our study focuses on demonstrating an APD operating in the eye-safe short-wave infrared (SWIR) spectrum (>1400 nm) with high multiplication ($M > 1200$) and low excess noise ($F < 7$ at $M = 200$) at room temperature. This device utilizes GaAsSb and $\text{Al}_{0.85}\text{Ga}_{0.15}\text{AsSb}$ in a separate absorber, charge, and multiplication (SACM) configuration on an InP substrate. Notably, this device exhibits more than 40 times improvement in maximum achievable multiplication and 6.5 times lower excess noise at $M = 25$ compared to commercially available InGaAs/InP devices.

Keywords: Avalanche photodiode (APD), excess noise, avalanche multiplication, impact ionization, 1550 nm, AlGaAsSb,

2. INTRODUCTION

Photodetectors operating within the short-wave infrared (SWIR) spectrum find extensive use in civilian applications like LiDAR and free space communication. For SWIR applications with limited photon availability, avalanche photodiodes (APDs) are commonly used to improve overall system sensitivity. These APDs enhance sensitivity by employing internal multiplication (M) through the impact ionization process. Due to the randomness in the spatial position of impact ionization in semiconductors, this M is usually accompanied by an extra noise term called 'excess noise'. McIntyre's local field theory defines this excess noise factor (F) using the equation¹:

$$F(M) = kM + (1-k)(2-1/M) \quad (1)$$

Here ' k ' represents the ratio of ionization coefficients for holes (β) and electrons (α), denoted as $k = \beta/\alpha$ for the case when the multiplication is initiated by electrons. Excess noise sets a limit on the maximum useful multiplication achievable for a given device. Therefore, high-sensitivity APDs requiring a large signal-to-noise ratio (SNR), require the use of avalanche materials with a low ' k ' value. Additionally, materials with dissimilar ionization coefficients between electrons and holes reduce the number of transits of the multiplication region leading to not only lower noise but also improved bandwidth².

Silicon avalanche photodiodes (APDs) operating at wavelength in the visible and up to 950 nm are widely used due to their performance, sensitivity, reliability, and cost-effectiveness. The 1550 nm wavelength has however emerged as an

option for extended-distance applications owing to the reduced solar background radiation and scattering³ and the ability to utilize higher laser powers while maintaining eye safety. Traditional APDs designs for 1550 nm operation rely on a structure with a narrow bandgap material, such as InGaAs for absorption, and a wide bandgap material for multiplication region, grown on an InP substrate. These alloys are integrated into a separate absorber, charge, and multiplier (SACM) configuration. The electric field in the absorber is deliberately kept low to minimize tunnelling current and impact ionization, while a high electric field in the multiplication region provides enough energy for impact ionization to occur. Commercially available linear mode APDs operating at 1550 nm utilize InP or InAlAs as the multiplication region and InGaAs as the absorber within a SACM structure. However, the maximum useful multiplication is restricted by high excess noise ($F > 10$ at $M=25$)⁴ due to similar ionization coefficients between electrons (α) and holes (β) at high electric fields^{5,6}, limiting its performance.

HgCdTe and InAs have demonstrated very low excess noise at 1550 nm, but they need cooled operation to reduce the dark current due to their small bandgap^{7,8}. AlInAsSb lattice-matched to GaSb exhibits low excess noise performance at room temperature beyond 1500 nm⁹. But this alloy requires complicated digital alloy growth techniques. Yi *et al.* showed very low excess noise equivalent to a k value of 0.005 in a 1550 nm AlAsSb $p-i-n$ structure¹⁰. However, the high Al content in this alloy leads to oxidation. Al_{0.85}Ga_{0.15}AsSb (hereafter AlGaAsSb) has demonstrated reduced surface dark currents and very low excess noise characteristics^{11,12}. By combining AlGaAsSb with either an InGaAs^{13,14} or GaAsSb^{15,16} absorber, it has achieved very high sensitivity at 1550 nm along with high bandwidth¹⁷. Lee *et al.*¹⁶ demonstrated that GaAsSb/AlGaAsSb can achieve a high gain of 278 at room temperature with excess noise $F < 3$ at $M=60$. Utilizing GaAsSb instead of InGaAs enables the conduction and valence bands energy level to change smoothly from the GaAsSb absorber to the AlGaAsSb multiplier region without a significant bandgap discontinuity. This facilitates easier carrier extraction, minimizing trapping and enhancing device speed. In contrast, InGaAs, with its type II band alignment, presents a larger conduction band offset ($\sim 1\text{eV}$) between the last grading layer and the AlGaAsSb multiplier. This work has employed a similar design by using GaAsSb as the absorber and AlGaAsSb as multiplication region, but the charge sheet has been optimized to further improve the performance of the device compared to ref [16] by reducing the electric field in the absorber region. The maximum multiplication in this work has been improved to $M=1212$ and excess noise $F < 7$ at $M=200$.

3. GROWTH AND FABRICATION

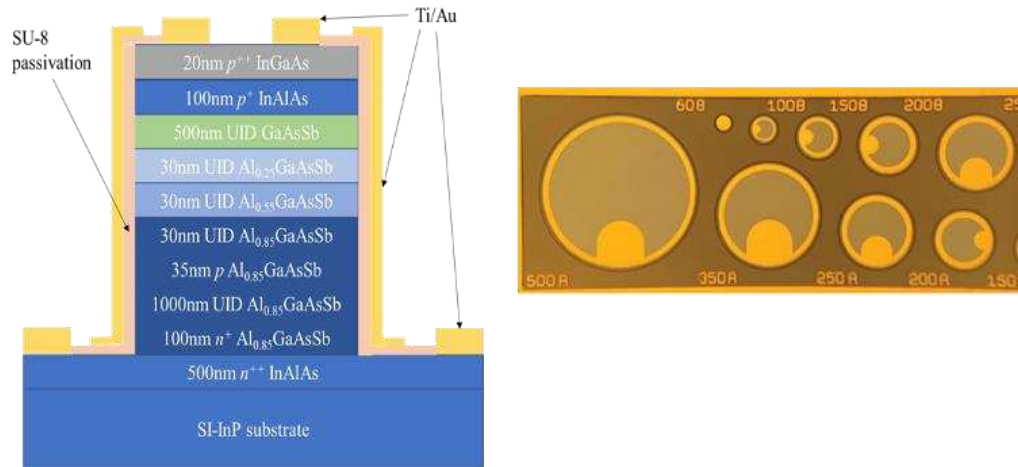


Figure 1. a) A schematic structure of GaAsSb/AlGaAsSb SACM APD. b) Microscope image of the fabricated devices. Numbers indicate the diameter of the devices in μm .

The GaAsSb/AlGaAsSb SACM APDs were grown via molecular beam epitaxy on a semi-insulating InP substrate using random alloy (RA) growth technique. For the group V cells, RIBER VAC 500 and Veeco Mark V valved crackers were employed for As and Sb, respectively. As depicted in Figure 1, this structure included a nominal 500 nm GaAsSb absorber and 1000 nm AlGaAsSb, incorporating a 35 nm charge sheet layer with p -type doping of $6 \times 10^{17} \text{ cm}^{-3}$. This doping ensures a low electric field in the absorber, preventing tunneling, while maintaining a high electric field in the multiplication region to facilitate avalanche multiplication. The energy bands are graded using various compositions of AlGaAsSb to enable smooth carrier migration from the absorber to the multiplication region. Device fabrication involved standard photolithography and wet etching in a solution composed of 40 ml citric acid:10ml phosphoric acid:10ml H_2O_2 :240 ml

deionized water. This process etches the devices into a clear mesa shape with diameters ranging from 60 μm to 500 μm , and the surface was passivated using SU-8. Ti/Au was deposited on the top and bottom contact layers for ohmic contact.

4. METHOD AND RESULTS

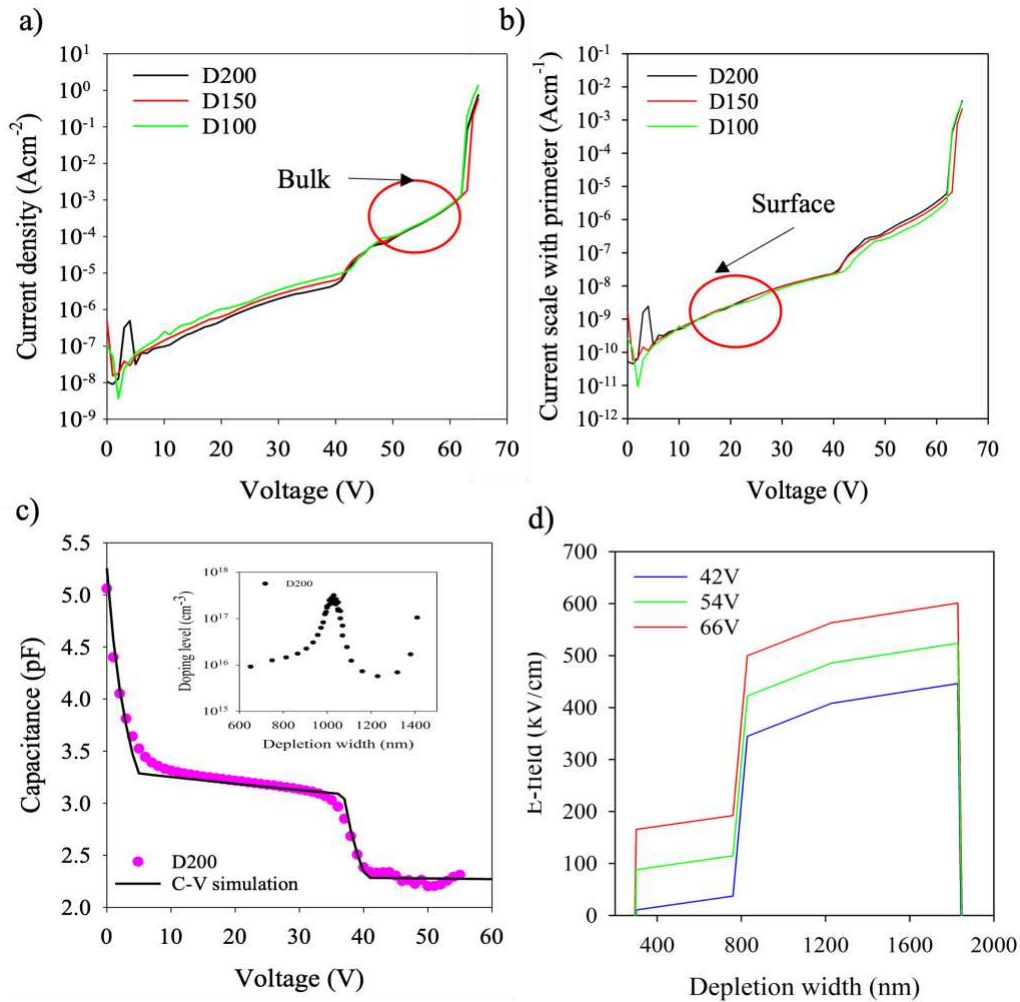


Figure 2: a) Different size devices dark current scale with area. b) Different size devices dark current scale with perimeter. c) Capacitance–voltage measurements on 200 μm device (insert is the doping profile). d) Electric field simulation at punch-through voltage and breakdown voltage.

Different size devices dark current scale with area and perimeter as shown in figure 2a and 2b respectively. The dark current scale with area better than perimeter after punch-through. This indicates that the dark current is limited by generation and recombination in the narrow bandgap material, whereas surface leakage current dominates the dark current before punch-through when only the wide bandgap multiplication region is depleted. The avalanche breakdown voltage (V_{bd}) is about 66 V while punch-through voltage (V_{pt}) is 42 V. There is small variation in breakdown and punch-through voltage due to edge breakdown and uniformity across the wafer. Figure 3c shows the capacitance with increasing reverse bias, with the clear punch-through of the electric field into the absorption layer occurring at around 42 V. A 1-D simulation based on Poisson's equation suggested that absorber and multiplication region thickness are 460 nm and 1060 nm respectively. The charge sheet thickness is 68nm with p -type doping of $3.5 \times 10^{17} \text{ cm}^{-3}$. The total charge in this charge sheet increased to $2.5 \times 10^{12} \text{ cm}^{-2}$ compared to previously reported $2.1 \times 10^{12} \text{ cm}^{-2}$ ¹⁶, leading to a significant improvement in the device performance. Figure 1d shows the electric field distribution in this SACM APD, the AlGaAsSb multiplication region exhibit an electric field over 600 kV/cm at breakdown voltage to provide large avalanche multiplication whereas

GaAsSb absorber experience a low electric field (<180 kV/cm) region to minimize the tunnelling leakage current. The tunnelling threshold is similar to InGaAs because of similar bandgaps and electron-effective mass¹⁸.

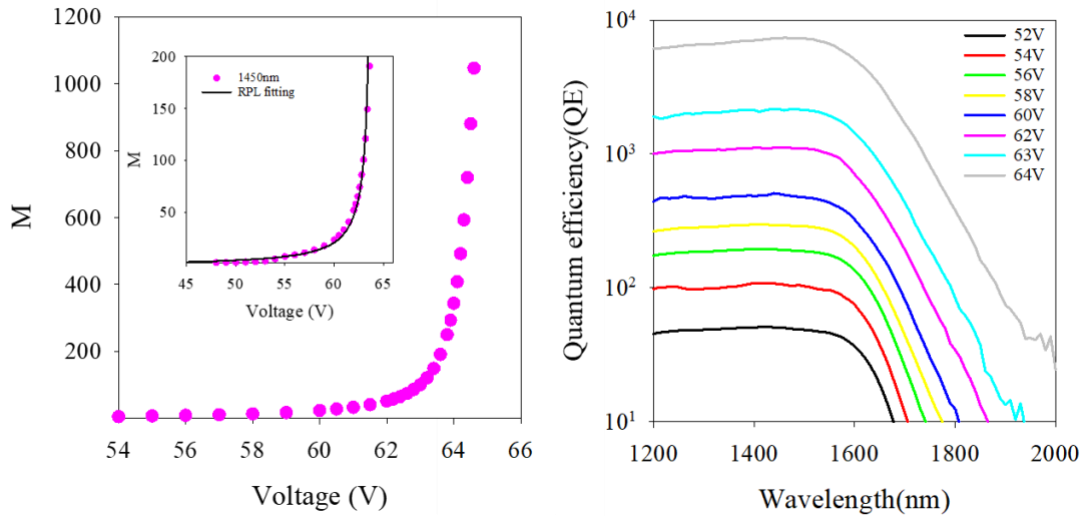


Figure 3: a) Avalanche multiplication for SACM APD at 1450nm (insert: RPL model fitting). b) External quantum efficiency (EQE) of SACM APD at different reverse bias.

Figure 3a illustrates the avalanche multiplication at different reverse biases for SACM APD operating at 1450 nm. The device was illuminated with a Thorlabs fiber coupled LED (M1450F1)¹⁹ with a phase sensitive technique at 180Hz to eliminate the DC dark current. Under illumination, only electrons generated in the *p*-type absorber region travel to the high-field region for impact ionization. The multiplication of the SACM APD at a given voltage was determined by comparing the absolute photocurrent value to that of a GaAsSb *p-i-n* diode with an identical optical sensing area at unity gain, calculating the differences in photo current. A random path length (RPL) model²⁰ was used to calculate SACM APD's multiplication with electric field distribution profile obtained from CV modeling (as depicted in figure 2d) and the impact ionization coefficient of AlGaAsSb²¹ published previously. This multiplication is determined to be $M=5$ at 54 V, and the modelled multiplication at voltages from 54 V onwards agree well up to a $M=1212$ with the measured photocurrent results shown in figure 2b (insert). In figure 3b, the quantum efficiency (QE) spectra was measured by focusing the light from a 100W tungsten bulb source through a monochromator. Using a phase-sensitive technique, the photocurrent was measured, and the responsivity was calculated by calibrating the monochromator output power with an InGaAs photodiode (FD05D)²². At 1450 nm, the external quantum efficiency at unity gain was measured to be 21.35% without anti-reflection (AR) coating. However, with maximum multiplication ($M=1212$), this device was capable of achieving a quantum efficiency as high as 25876%.

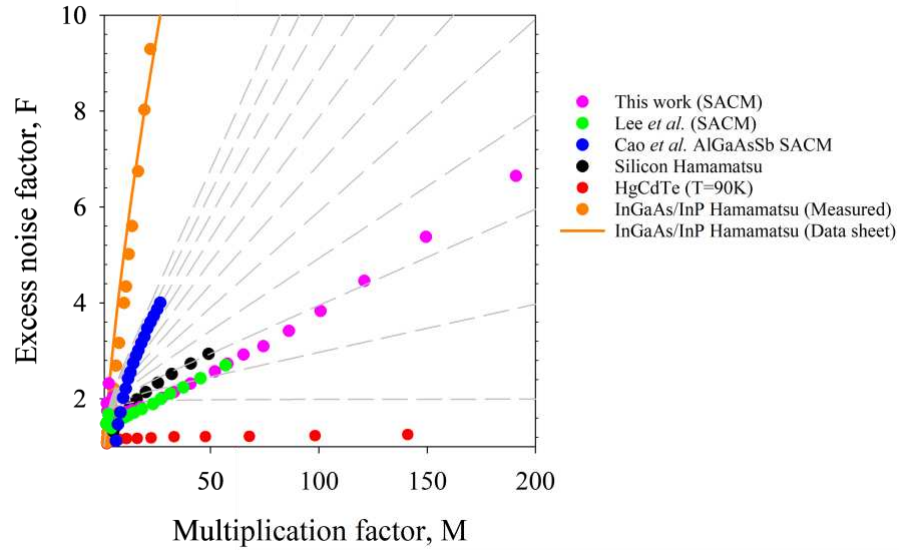


Figure 4: Excess noise factor as function of the multiplication. Green circle represents GaAsSb/AlGaAsSb SACM APD by Lee *et al*¹⁶; Black circle represents Silicon APD by Hamamatsu²³; Blue circle represents InGaAs/AlGaAsSb SACM APD by Cao *et al.* from Huawei.²⁴; Orange circle represents InGaAs/InP SACM APD by Hamamatsu⁴.

The excess noise measurements were performed using a transimpedance amplifier-based circuit with a centre frequency of 10MHz and a bandwidth of 4.2MHz²⁵. The shot noise was calibrated by using a reference device (SFH2701 silicon photodiode²⁶) without multiplication. The measured noise power of the SACM APD was compared to the measured noise power of the silicon device at a given photocurrent to determine the excess noise factor. In Figure 4, the excess noise was measured up to $M=200$ which yield an excess noise factor $F < 7$. Since most of impact ionization occurs in the high field 1000 nm AlGaAsSb multiplication region, the excess noise results agree well with AlGaAsSb 1000 nm *p-i-n* device²⁷. This work shows similar excess noise to Lee *et al.*¹⁶ due to similar thickness and alloy composition of the multiplication region, but this work measures the excess noise up to $M=200$. Cao *et al.* from Huawei reported a similar InGaAs/AlGaAsSb SACM APD is capable of 50 Gb/s operation²⁴, but the excess noise is almost 2 times higher than this work. A Hamamatsu InGaAs/InP 1550 nm device was measured to show an excess noise of 10 at $M=30$ (orange symbol) agreeing well with their data sheet⁴. Our device therefore shows at least 6.5 times improvement in excess noise compared to a commercial InGaAs/InP APD at $M=25$ and is even lower than that of a low noise commercial Si APD²⁸. This improvement in excess noise compared to InP or InAlAs SACM APDs is because the addition of large Sb atoms into AlGaAs modifies the valance band structure¹⁶, increasing the spin-orbit splitting energy and reducing the possibility of hole ionization. More recently, Lewis *et al.* showed that in AlGaAsSb, the ionisation probability density function (PDF) is in fact peaked, and follows a Weibull-Frechet shape, reducing the F further²⁷.

Table 1: A summary of GaAsSb/AlGaAsSb device parameters compared with other commercial devices.

Parameters	Excelitas (C30662)	Hamamatsu (G8931-20)	Hamamatsu (G14858-0020AA)	AlGaAsSb SACM (Lee <i>et al.</i>)	SACM (This work)
Device diameter	200 μm	200 μm	200 μm	200 μm	200 μm
Spectrum range	$\sim 1.7\mu\text{m}$	$\sim 1.7\mu\text{m}$	$\sim 1.7\mu\text{m}$	$\sim 1.7\mu\text{m}$	$\sim 1.7\mu\text{m}$
Capacitance@Max Depletion	2.5pF	1.5pF	2 pF	2 pF	2 pF
Breakdown Voltage	50V	55V	65 V	70 V	66V
C_{bd}	140mV/K	110 mV/K	100 mV/K	11.83 mV/K	N/A
Bandwidth	0.85GHz	0.9GHz	0.9 GHz	0.7 GHz	N/A
Max Multiplication	~ 20	~ 30	~ 30	~ 278	1212
Excess noise @ $M = 25$	3.4@M=1 0	~ 13	~ 13	~ 2	~ 2
Dark current @ $M = 25$	4.5nA@M =10	2280nA	20nA	480nA	214nA

In Table 1, a comparison is drawn between the GaAsSb/AlGaAsSb SACM APD and other commercially available InGaAs APDs with a 200 μm diameter. The state-of-the-art InGaAs/InP device (G14858-0020AA)⁴ exhibits low dark current and a similar breakdown voltage compared to the presented work. However, this work demonstrates the capability to achieve a remarkably high multiplication factor of 1212, almost 30 times higher than that device, while keeping the excess noise 6.5 times lower at $M=25$ in comparison. Comparing this work to the study by Lee *et al*¹⁶, the excess noise remains similar due to same material systems employed. However, improvements in charge sheet design have resulted in four times increase in the maximum achievable multiplication and a reduction in dark current by a factor of two because of reduced tunneling current. The thin GaAsSb absorber (500 nm) yields a quantum efficiency (QE) of 21.35% at unity gain without anti-reflection (AR) coating. However, using a 2 μm thick GaAsSb absorber in the SACM configuration with AR coating could enhance this to 87% at unity gain with only a small increase in dark current and a slightly lower speed. More recently, Jin *et al.* showed that a 1550 nm thick $\text{Al}_{0.75}\text{Ga}_{0.25}\text{AsSb}$ *p-i-n* diode achieved an even lower excess noise of $F=2.4$ at $M=90$ ³⁰. By integrating a thicker InGaAs or GaAsSb absorber in a SACM structure with such a multiplication region may yield an even better performance.

5. CONCLUSION

In summary, this study presents a GaAsSb/AlGaAsSb SACM APD that is lattice-matched to InP, showing high gain and low excess noise. This device significantly improves the overall sensitivity for 1550nm detection compared to state-of-the-art commercial APDs. Building upon prior work by Lee *et al*¹⁶, this research achieves a maximum achievable multiplication of $M=1212$ by optimizing the charge sheet to yield lower dark current.

6. REFERENCE

- [1] McIntyre, R. J., "Multiplication noise in uniform avalanche diodes," *IEEE Trans. Electron Devices* **ED-13**(1), 164–168 (1966).
- [2] Emmons, R. B., "Avalanche-Photodiode Frequency Response," *J. Appl. Phys.* **38**(9), 3705–3714 (1967).
- [3] Gueymard, C. A., "Parameterized transmittance model for direct beam and circumsolar spectral irradiance," *Sol. Energy* **71**(5), 325–346 (2001).
- [4] Hamamatsu., "Hamamatsu product datasheet: InGaAs APD (G14858-0020AA)," Ichino-cho (2010).
- [5] Tan, L. J. J., Ng, J. S., Tan, C. H. and David, J. P. R. R., "Avalanche noise characteristics in submicron InP diodes," *IEEE J. Quantum Electron.* **44**(4), 378–382 (2008).
- [6] Goh, Y. L., Marshall, A. R. J., Massey, D. J., Ng, J. S., Tan, C. H., Hopkinson, M., David, J. P. R., Jones, S. K., Button, C. C. and Pinches, S. M., "Excess avalanche noise in In_{0.52}Al_{0.48}As," *IEEE J. Quantum Electron.* **43**(6), 503–507 (2007).
- [7] Ker, P. J., Marshall, A. R. J., David, J. P. R. R. and Tan, C. H., "Low noise high responsivity InAs electron avalanche photodiodes for infrared sensing," *Phys. Status Solidi Curr. Top. Solid State Phys.* **9**(2), 310–313 (2012).
- [8] Finger, G., Eisenhauer, F., Genzel, R., Mandla, C., Baker, I., Alvarez, D., Amorim, A., Brandner, W., Dupuy, C., Deen, C., Ives, D., Mehrgan, L., Meyer, M., Perraut, K., Perrin, G., Stegmeier, J., Straubmeier, C., Weller, H. J. and Isgar, V., "Scientific detector workshop 2022 on-sky performance verification of near-infrared e-APD technology for wavefront sensing and demonstration of e-APD pixel performance to improve the sensitivity of large science focal planes," *Astron. Nachrichten*, e20230069 (2023).
- [9] Jones, A. H., March, S. D., Bank, S. R. and Campbell, J. C., "Low-noise high-temperature AlInAsSb/GaSb avalanche photodiodes for 2- μ m applications," *Nat. Photonics* **14**(9), 559–563 (2020).
- [10] Yi, X., Xie, S., Liang, B., Lim, L. W., Cheong, J. S., Debnath, M. C., Huffaker, D. L., Tan, C. H. and David, J. P. R., "Extremely low excess noise and high sensitivity AlAs_{0.56}Sb_{0.44} avalanche photodiodes," *Nat. Photonics* **13**(10), 683–686 (2019).
- [11] Lee, S., Kodati, S. H., Guo, B., Jones, A. H., Schwartz, M., Winslow, M., Grein, C. H., Ronningen, T. J., Campbell, J. C. and Krishna, S., "Low noise Al_{0.85}Ga_{0.15}As_{0.56}Sb_{0.44}avalanche photodiodes on InP substrates," *Appl. Phys. Lett.* **118**(8), 0–5 (2021).
- [12] Lee, S., Guo, B., Kodati, S. H., Jung, H., Schwartz, M., Jones, A. H., Winslow, M., Grein, C. H., Ronningen, T. J., Campbell, J. C. and Krishna, S., "Random alloy thick AlGaAsSb avalanche photodiodes on InP substrates," *Appl. Phys. Lett.* **120**(7), 071101 (2022).
- [13] Collins, X., White, B., Cao, Y., Osman, T., Taylor-Mew, J., Ng, J. S. and Tan, C. H., "Low-noise AlGaAsSb avalanche photodiodes for 1550nm light detection," 4 March 2022, 16, *SPIE-Intl Soc Optical Eng.*
- [14] Collins, X., Sheridan, B., Price, D., Cao, Y., Blain, T., Ng, J. S., Tan, C. H. and White, B., "Low-noise AlGaAsSb avalanche photodiodes for 1550 nm light detection," *Proc.SPIE* **12417**, 124170K (2023).
- [15] Cao, Y., Blain, T., Taylor-Mew, J. D., Li, L., Ng, J. S. and Tan, C. H., "Extremely low excess noise avalanche photodiode with GaAsSb absorption region and AlGaAsSb avalanche region," *Appl. Phys. Lett.* **122**(5), 51103 (2023).
- [16] Lee, S., Jin, X., Jung, H., Lewis, H., Liu, Y., Guo, B., Kodati, S. H., Schwartz, M., Grein, C., Ronningen, T., Campbell, J., David, J. and Krishna, S., "High Gain, Low Noise, Room Temperature 1550 nm GaAsSb/AlGaAsSb Avalanche Photodiodes," *Optica* (2022).
- [17] Ie, S. H. X., Hou, X. I. Z., Hang, S. H. Z., Homson, D. A. J. T., Ia, X., Hen, C., Eed, G. R. T. R., Hien, J. O. S. N. G., An, C. H. E. E. H. I. N. G. T., So, S., Xie, S., Zhou, X., Zhang, S., Thomson, D. J., Chen, X., Reed, G. T., Ng, J. S. and Tan, C. H., "InGaAs/AlGaAsSb avalanche photodiode with high gain-bandwidth product," *Opt. Express* **24**(21), 24242 (2016).
- [18] Jung, H., Lee, S., Liu, Y., Jin, X., David, J. P. R. and Krishna, S., "High electric field characteristics of GaAsSb photodiodes on InP substrates," *Appl. Phys. Lett.* **122**(22), 221102 (2023).
- [19] Wavelength, N., Size, E., Power, E., Lifetime, T., Temperature, S. and Group, R., "Fiber-Coupled LED, 1450 nm" (2022).
- [20] Ong, D. S., Li, K. F., Rees, G. J., David, J. P. R. and Robson, P. N., "A simple model to determine multiplication and noise in avalanche photodiodes," *J. Appl. Phys.* **83**(6), 3426–3428 (1998).
- [21] Guo, B., Jin, X., Lee, S., Ahmed, S. Z., Jones, A. H., Xue, X., Liang, B., Lewis, H. I. J., Kodati, S. H., Chen, D., Ronningen, T. J., Grein, C. H., Ghosh, A. W., Krishna, S., David, J. P. R. and Campbell, J. C., "Impact Ionization Coefficients of Digital Alloy and Random Alloy Al_{0.85}Ga_{0.15}As_{0.56}Sb_{0.44} in a Wide Electric Field Range," *J. Light. Technol.* **40**(14), 4758–4764 (2022).
- [22] Range, W., Wavelength, P., Diameter, A. A., Material, S., Ratings, A. M., Temperature, O. and Temperature, S., "InGaAs Photodiode FD05D Photodiode Responsivity Responsivity (A / W)" (2017).
- [23] Hamamatsu., "Hamamatsu product data sheet (Silicon APD S10341)" (2018).
- [24] Cao, J., Xiang, W., Wang, K., Wei, W., Zhang, S. and Teng, Y., "Communication of HUAWEI RESEARCH" (2023).
- [25] Green, J. E., David, J. P. R. and Tozer, R. C., "A transimpedance amplifier for excess noise measurements of high junction capacitance avalanche photodiodes," *Meas. Sci. Technol.* **23**(12), 1–24 (2012).
- [26] OSRAM data sheet., "High Speed PIN-Photodiode(SFH2701)," Regensburg (2008).

- [27] Lewis, H. I. J., Jin, X., Guo, B., Lee, S., Jung, H., Kodati, S. H., Liang, B., Krishna, S., Ong, D. S., Campbell, J. C. and David, J. P. R., “Anomalous excess noise behavior in thick Al_{0.85}Ga_{0.15}As_{0.56}Sb_{0.44} avalanche photodiodes,” *Sci. Rep.* **13**(1), 9936 (2023).
- [28] Hamamatsu., “Hamamatsu product data sheet (Silicon APD S16453 short wavelength type APD),” Ichino-cho (2018).
- [29] Liu, Y., Yi, X., Bailey, N. J., Zhou, Z., Rockett, T. B. O., Lim, L. W., Tan, C. H., Richards, R. D. and David, J. P. R., “Valence band engineering of GaAsBi for low noise avalanche photodiodes,” *Nat. Commun.* **12**(1) (2021).
- [30] Jin, X., Lewis, H. I. J., Yi, X., Xie, S., Liang, B., Tian, Q., Huffaker, D. L., Tan, C. H. and David, J. P. R., “Very low excess noise Al_{0.75}Ga_{0.25}As_{0.56}Sb_{0.44} avalanche photodiode,” *Opt. Express* **31**(20), 33141–33149 (2023).

7. FUNDING AND ACKNOWLEDGEMENT

This work was supported by the Advanced Component Technology (ACT) program of NASA's Earth Science Technology Office (ESTO) under grant NO. 80NSSC21K0613.; Engineering and Physical Sciences Research Council (EP/R513313/1). X.J, Y.L S. L and H.J contributed to optimizing the structure design. X.J, Y.L undertook IV, CV, QE, multiplication, excess noise for SACM APD device. S.L and H.J performed material growth, fabrication. All authors reviewed and approved the manuscript.